

## Technical Note SCD 3

# Electron Beam Profiles on a Rotating Anode and the Consequences for the X-ray Intensity

### Introduction

Power density (or power loading) is widely used as a measure of the performance of X-ray sources. The reason for this is intuitively obvious; for a given source, the total X-ray flux is indeed proportional to the power density applied to the anode. However, we will show that for comparing different sources, power density is a poor predictor of relative performance since differences in the anode focal spot distribution can have very large effects on the intensity of the X-ray beam. Indeed, differences in spot shape can lead to a full factor of four difference in intensity for the same power density. This makes it difficult to compare different X-ray sources. It is, therefore, more informative to evaluate the crystallographic data obtained from the same sample on different X-ray sources. For this reason, Bruker AXS is the first manufacturer to routinely publish absolute specifications for X-ray beam intensity.

The corollary to this observation is that careful optimization of the electron beam focus can yield very significant improvements in performance. The new MICROSTAR ULTRA is the first rotating anode design which takes into account fully the optimization of the anode focal spot distribution (patent pending) and is thus able to achieve significantly higher X-ray beam intensity than conventional rotating anode designs.

To see the influence of the electron beam profile on the resulting X-ray beam profile, two independent simulations have been performed. The production of X-rays has been simulated from the electron beam profile on the rotating anode through the X-ray optic to the crystal position in the focus of the optic.

First, the flash temperature on the anode is calculated using a finite difference program. The flash temperature is the maximum temperature increase due to the electrons. The program calculates the temperature on the rotating anode in three dimensions using the real material and anode properties. The anode is a copper anode with a diameter of 89 mm, rotating at 6000 rpm. The power on the anode was modified to get a flash temperature of 800 K. The outcome of these calculations is the power distribution on the anode.

With the calculated power distributions, a source for X-rays is obtained. The second simulation is the ray tracing of X-rays from the X-ray source through the optic to the crystal position. The simulated optic is the MONTEL 200 multilayer mirror. The distance from the source to the middle of the optic is 120 mm. The Bragg line of the multilayer is modeled as a Gaussian profile. The line position on the  $\theta$ -axis changes over the length of the optic according to the angle of the central ray. For each

position in the crystal plane rays are traced back to the optic and from the optic to the source, where the relative contribution of the flux in this point in the crystal plane is calculated. Thus a flux profile is obtained.

### Peak Profiles and Anode Flash Temperature

Three different beam profiles were simulated; all profiles have the same FWHM of 100  $\mu\text{m}$ :

A block profile given by:

$$P(s) = \begin{cases} 0 & \text{if } r > FWHM \\ I_0/2 & \text{if } r = FWHM \\ I_0 & \text{if } r < FWHM \end{cases} \quad (1)$$

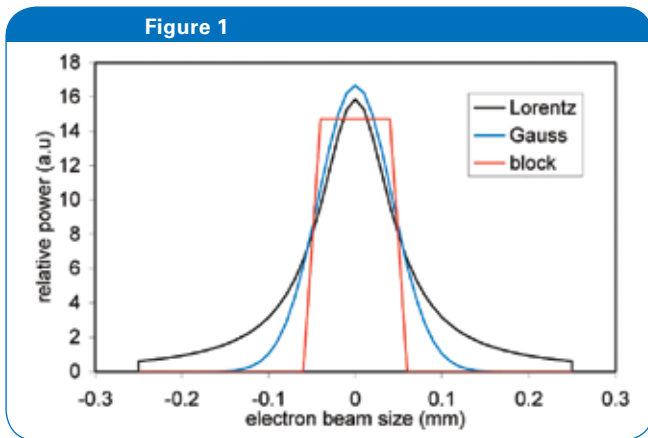
A Gaussian profile given by:

$$P(s) = \begin{cases} 0 & \text{if } r > \text{boundary} \\ I_0 \exp(-r^2/2\sigma^2) & \text{if } r < \text{boundary} \end{cases} \quad (2)$$

A Lorentzian profile given by:

$$P(s) = \begin{cases} 0 & \text{if } r > \text{boundary} \\ I_0/(1+r^2/\sigma^2) & \text{if } r < \text{boundary} \end{cases} \quad (3)$$

The boundary of the calculation is set at 250  $\mu\text{m}$ . This boundary has no influence on the block profile, but cuts the other profiles to zero at  $r = 250 \mu\text{m}$ . This has been done in the whole calculation, so the only consequence is that the profiles used are not perfect Gaussian or Lorentzian. To calculate the temperature profile on the anode, the spot is stretched horizontally to make elliptical spots of  $0.1 \times 1 \text{mm}^2$ . The profiles as given by the above equations are as seen under the take-off angle of about  $6^\circ$ . The profiles in Figure 1 show 2-dimensional cuts through the center of these 3-dimensional profiles.



Electron beam profiles on a rotating anode giving a flash temperature of 800K

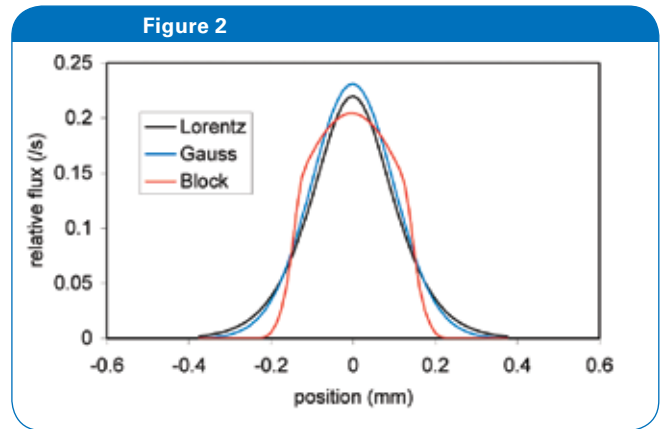
In this figure, the profiles are scaled such that they give the same flash temperature on the anode. The consequence would be that these three electron beams would roughen the anode by the same amount. The electron powers under the 3-d profiles to reach a flash temperature of 800K are given in the table below. In the table the peak parameters as used in equations 1 to 3 are also given.

Table 1: Electron beam profile parameters.

profile	Power (W)	$l_0$	$\sigma$ ( $\mu\text{m}$ )
Lorentz	4376	15.88	50.00
Gauss	1890	16.68	42.47
Block	1106	14.74	

### X-ray Tracing

The next step is the tracing from source to crystal plane. A 2-dimensional cut through these profiles is plotted in Figure 2. The shown cuts are in the horizontal direction. Due to the (lack of) symmetry of the setup there is only vertical symmetry, left right is influenced by the small difference in distance from the left or the right side of the crystal to the optic.



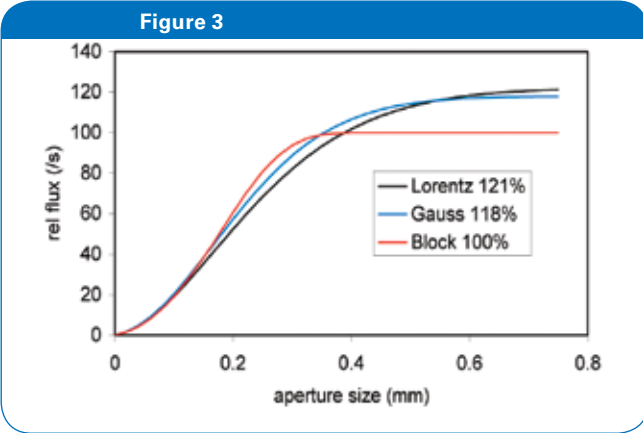
2-dimensional cut through the X-ray flux distribution in the plane of the crystal.

In table 2, the FWHM of the various profiles in the horizontal and vertical directions are given.

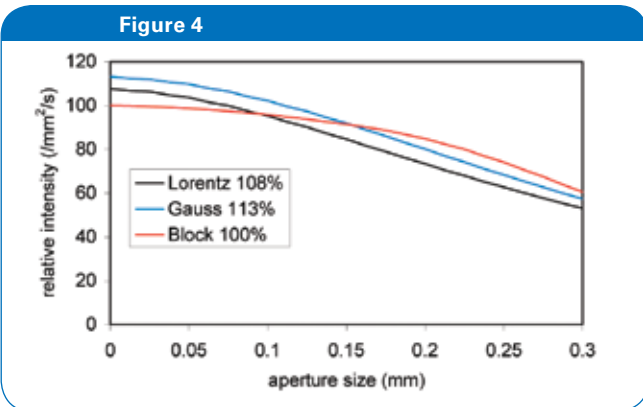
Table 2: FWHM of the X-ray beam depending on the electron beam profile.

Profile	FWHM hor (mm)	FWHM ver (mm)
Lorentz	0.22730	0.22763
Gauss	0.23679	0.23677
Block	0.28190	0.28191

From the obtained flux distribution data the intensity and flux as function of the aperture size can be obtained. A different way to look at this is by having a crystal of the size and measure the flux through it and for the intensity divide it through the area of the crystal. The results are plotted in Figures 3 and 4.



Relative flux as a function of the crystal size. The differences in flux for small crystals are difficult to see. Only for large crystals the flux of the Lorentz profiles is the highest.



Relative intensity as a function of the crystal size. It is clear that for crystals smaller than 150  $\mu\text{m}$  a Gaussian profile is best.

Table 3 summarizes the output of these calculations. As can be seen there is no correlation between power density based on FWHM, flux and intensity. It is also not possible to find a correlation when the power density would be based on the full width at a different height e.g. 10% maximum.

Table 3: Relation between power density, maximum flux and maximum intensity for a rotating anode of which the flash temperature was set to 800K.

Profile	Power density (kW/mm <sup>2</sup> )	max Flux /s (%)	max Intensity /s /mm <sup>2</sup> (%)
Lorentz	43.76	396	121
Gauss	18.90	171	118
Block	11.46	100	100

### Conclusions

Table 3 shows that with a fixed flash temperature of the rotating anode, the power density can vary by a factor of four depending on the peak shape. The resulting X-ray beam quality is almost the same for these three completely different power densities. The only time that X-ray beam quality can be compared via the power density is when the electron beam profiles on the anode are the same.

The consequence is also that for a given power loading, the intensity of an X-ray source may vary by up to a factor of four depending on the shape and distribution of the anode spot focus. Because of this, careful optimization of the anode focus can yield very significant improvements in source performance. The MICROSTAR ULTRA is the first source to employ a fully optimized electron focus design (patent pending) and is thus able to produce a significantly more intense beam than conventional rotating anodes.

Also, because of the impact of the anode focus shape on beam intensity, it is not possible to compare the relative performance of X-ray sources based on power loading alone. Rather, the sources should be compared by direct measurements of X-ray intensity at the sample position.

All configurations and specifications are subject to change without notice. Order No. DOC-T86-EXS003. © 2007 Bruker AXS. Printed in the United States.

● **Bruker AXS Inc.**

Madison, WI, USA  
Phone +1 (800) 234-XRAY  
Phone +1 (608) 276-3000  
Fax +1 (608) 276-3006  
info@bruker-axs.com  
www.bruker-axs.com

**Bruker AXS GmbH**

Karlsruhe, Germany  
Phone +49 (721) 595-2888  
Fax +49 (721) 595-4587  
info@bruker-axs.de  
www.bruker-axs.de

**Bruker AXS BV**

Delft, The Netherlands  
Phone +31 (152) 152 400  
Fax +31 (152) 152 500  
info@bruker-axs.nl  
www.bruker-axs.nl